Journal of Thermal Analysis and Calorimetry, Vol. 89 (2007) 2, 595–600

PRODUCTION OF BSCCO BULK HIGH T_c SUPERCONDUCTORS BY SOL–GEL METHOD AND THEIR CHARACTERIZATION BY FTIR AND XRD TECHNIQUES

M. Arshad [1]*, *A. H. Qureshi* [2], *K. Masud* [3] *and N. K. Qazi* [2]

[1]APD, PINSTECH, Nilore, Islamabad, Pakistan
[2]NMD, PINSTECH, Nilore, Islamabad, Pakistan
[3]P.O. Box 27, CPC, Project, D.G. Khan, Punjab, Pakistan

The production of bulk high T_c superconducting phase (2223) by EDTA-gel (ethylenediaminetetraacetic acid) techniques has been investigated. It is shown that close control of pH is necessary for the production of a well-complexed precursor which allows subsequent decomposition in two stages at 300 and 800°C. The problem of carbonate formation was investigated experimentally and solved. Precursors are characterised by Fourier transform infrared (FTIR) spectroscopy and X-ray diffraction (XRD) and the sintering behaviour was monitored by dilatometry. At least three different phases $Bi_2Sr_2Ca_{x-1}Cu_xO_{8+y}$ (BSCCO); where x=1, 2, 3 were identified within superconducting pellets using XRD, named as $Bi_2Sr_2CuO_7$ (2201), $Bi_2Sr_2CaCu_2O_9$ (2212) and $Bi_2Sr_2Ca_2Cu_3O_{10}$ (2223). The superconducting properties of the sintered samples were studied by vibrating sample magnetometer (VSM). Transition to a superconducting state around 80 K appeared in samples (sintered at 845°C) containing the $Bi_2Sr_2Ca_1Cu_2O_y$ (2212) phase. Liquid phase sintering of the samples aided the formation of $Bi_2Sr_2Ca_2Cu_3O_x$ (2223) phase at high temperature (860°C), which showed a superconducting transition temperature of 108 K.

Keywords: *BSCCO system, FTIR study, high T_c phase, pH effect, sol–gel technique, superconducting phases, XRD study*

Introduction

A number of intensive research efforts have been directed at improving the properties of bismuth-based superconductors soon after their discovery. It is evident that partial replacement of bismuth by lead (Pb) leads to enhance of superconducting properties such as J_c and T_c [1–9]. To augment the structural stability, to understand the nature of charge carriers, the effect of carrier concentration on the superconducting properties of the system, the substitution of different elements in the system and to study a number of related parameters are the subject of a number of communications, thus, playing a vital role and arousing much interest in this field [10–20].

Marcilly *et al*. [21] developed powder processing by pyrolysis of amorphous organic precursor. This solution process consists of mixing of the appropriate amount of ions, normally in the form of metallic salts such as nitrates or chlorides, and a polyfunctional hydroxy acid, e.g., citric acid [22–24] or EDTA [25–27]. Subsequent dehydration of the solution first yields the gel and then the amorphous precursor. The homogeneity of the aqueous solution of salts is preserved in the amorphous precursor and possibly retained in the final solid oxide product. The pH of initial aqueous solution is one of the most important factors affecting complex formation. Ammonium hydroxide is introduced into the precursor solution to aid pH adjustment and dissolution of metal salts. The sol–gel method involves chelation of cations with polyfunctional hydroxy acids such as citric acid and EDTA and polyesterification of excess polyfunctional acid with a polymorphic alcohol such as ethylene glycol or glycerol [28–32].

Sale *et al*. [33] showed the effect of Ba– in Y–Ba–Cu and La–Ba–Cu precursors to cause a stepwise decomposition which was associated with precipitation during gel formation. The decomposition of precursors has further been investigated by Baythoun *et al*. [22] and Delmon *et al*. [34]. Up to approximately 200°C dehydration occurs and then around 500°C the precursor decomposes/oxidises rapidly yielding a mixture of CO_2 and N_2O. In situations where the precursors contained Sr precipitates, the formation of $SrCO_3$ has been observed, which did not decompose until temperatures above 800°C. A common and important step in the fabrication of a wide range of oxide ceramics is the calcination stage. It is used to improve the processing characteristics in operations such as grinding, compaction and sintering, because the calcination products are aggregates of small crystallites.

---

* Author for correspondence: marshads53@yahoo.com.sg

1388–6150/$20.00
© 2007 Akadémiai Kiadó, Budapest

Akadémiai Kiadó, Budapest, Hungary
Springer, Dordrecht, The Netherlands

In addition, the release of volatile matter during calcination minimises internal shrinkage in later processing steps that can lead to the development of internal stresses and eventually crushing and warping [35]. To obtain a dense solid, the calcined powder requires to be pressed and subsequently sintered using either solid–solid or liquid phase diffusion processes.

In our earlier studies relating to the preparation and characterization of BSCCO and Pb–BSCCO system by sol–gel techniques, we also compared the volume-fraction of 2223 phase in both the systems [36]. This work is a continuation of the studies on BSCCO system and its related parameters [37]. The aim of the present investigation is to pursue a more detailed study on the effect of pH during the preparation of BSCCO bulk high T_c phase by the same method and its determination by infrared spectroscopy and X-ray diffraction techniques.

Experimental

The superconducting oxides were prepared using the amorphous gel route. This required high purity metal nitrates and organic acids which were acquired from Aldrich. For the production of gel, primary solution is prepared by dissolving metal nitrates in deionised water. $Bi(NO_3)_3$ does not dissolve in water forming a white precipitate of basic nitrate classically referred to as the 'magistery of bismuth flake/pearl white'.

$$Bi(NO_3)_3+2H_2O\text{ (excess)}\rightarrow Bi(OH)_2NO_3+2HNO_3$$

Therefore the addition of HNO_3 is required to dissolve bismuth nitrate. For each batch, a sufficient amount of organic acid (EDTA) was added for requisite complexation. EDTA does not dissolve in water at low pH (1–2), so the pH had to be raised by the addition of NH_4OH solution. A pH=6 was used to allow the organic acid to form organo–metallic complexes. The primary solution was converted into an amorphous gel using a rotary evaporator in a water bath at approximately 70°C and applying vacuum of a few tores. At this point it was poured into a Pyrex dish, placed in a vacuum oven and left for at least 12 h at 80°C and 10^{-1} tore. The precursor was dehydrated and a highly porous form with either glassy or foamy appearance resulted. The gel was converted into powder form by heating at 300 followed by 800°C each for 2 h. The pellets were produced by pressing the powder in press and then sintered at 845 and 860°C for different duration of time.

The investigation of complex and carbonates formation was carried out by Perkin Elmer 2000 FTIR spectrometer, which operates in the range of 450–6500 cm^{-1}. The powders at each stage, precursor, calcined and sintered states were characterised by powder X-ray diffraction using a Philips diffractometer coupled to a printing recorder and a computer with software for print-outs. The analyses were carried out at 40 kV and 20 mA. CuK_α, λ=1.5418 Ĺ was used as the X-ray source. The thermal stability of precursor and its decomposition products were studied by Seiko Simultaneous Thermal Analyzer (STA-409). A horizontal assembly dilatometer was applied for monitoring the sintering behavior of the pressed pellets of the calcined oxide powders. The superconductive transition temperatures were measured employing a Vibrating Sample Magnetometer (VSM)-3001, Oxford Instruments.

Results and discussion

FTIR spectrum

It was observed in our previous study by thermal analysis [36] that the decomposition process of the precursor was sharp and extremely exothermic. Therefore, to avoid vigorous heat evolution, burning and possible segregation, the precursor was heated in two stages at 300 and 800°C.

An FTIR spectrum of the EDTA gel, precursor heated at 300 and 800°C are shown in Figs 1a–c. In EDTA gel precursor (Fig. 1a) the absorption peaks due to carboxylate ions [38] were found at 637, 870 and 1602 cm^{-1}. The presence of the 1602 cm^{-1} band confirmed the complex formation in the BSCCO material. Only a few peaks due to NO_3^- ions were found at 1397, 853 and 825 cm^{-1}, which indicate that most of the ions were consumed to produce the precipitated NH_4NO_3 in the precursor during the gel processing. The presence of NH_4NO_3 as a crystalline phase in the precursor did not cause any problem of chemical

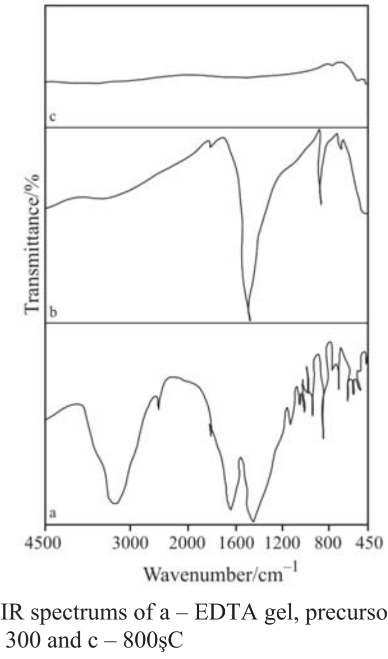

Fig. 1 FTIR spectrums of a – EDTA gel, precursor calcined at b – 300 and c – 800şC

Table 1 Species obtained in precursor calcined at 300°C

Wavenumber/ cm^{-1}	Species	Wavenumber/ cm^{-1}	Species
3436	water	1075	metal oxide
1777	carbonyl	874	$CaCO_3$
1506	carbonyl	858	$SrCO_3$
1472	carbonate	708	carbonate
1459	carbonate	517	metal oxide

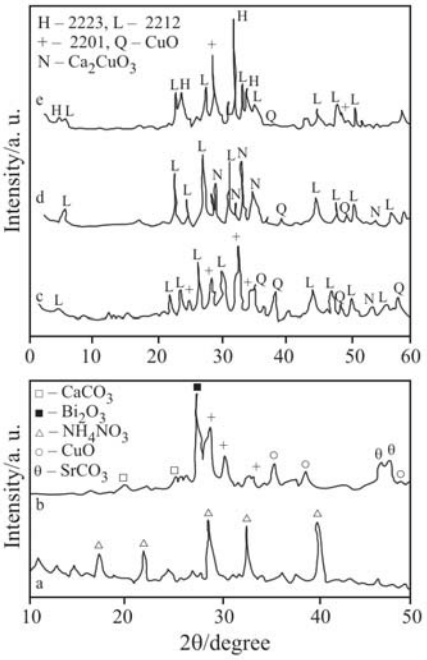

Fig. 2 XRD patterns of a – EDTA gel, precursor calcined at b – 300 and c – 800şC; d – sintered at 845şC for 60 h and e – 860şC for 60 h

inhomogeneity or agglomeration in the superconducting materials as never involved any of the metal ions required in the final product. The peaks for the carboxylic ion as well as the NO_3^- ion had disappeared (Fig. 1b) in the precursor heated at 300°C. A new band due to stretching vibration of the CO_3^{2-} appeared at 1459 cm^{-1}. Other peaks, which appeared and can be attributed to carbonates and metal oxide [39, 40] are shown in Table 1. It is known that carbonates form with an exothermic reaction in the temperature range of 250 to 500°C [41–43]. It is also known that in order to produce the superconducting phases from the gel, decomposition of the gel should be controlled to suppress the formation of carbonates of constituent species, since these carbonates give possible segregation and inhomogeneity in the final oxide powder. In order to avoid any carbonate formation, the precursor was heated continuously without intermediate cooling from 300 (2 h) to 800°C. An FTIR spectrum of a sample heated at 800°C is shown in Fig. 1c, which gives no evidence of carbonates in the oxide powder.

X-Ray diffraction

Figures 2a–e show an XRD patterns obtained from the EDTA gel, precursor heated at 300 and 800°C and pellets sintered at 845 and 860°C. The basic gel was amorphous but contained a significant amount of NH_4NO_3 as a crystalline phase (Fig. 2a). In the present study, the BSCCO sample required a large amount of nitric acid to dissolve the $Bi(NO_3)_3$ and ammonia to adjust the pH of the final solution of nitrates and EDTA, causing precipitation of the NH_4NO_3 during gel drying. It has been found that the formation of NH_4NO_3 is increased by excessive use of ammonia and nitric acid. XRD (Fig. 2b) of precursor heated at 300°C also confirmed the formation of carbonates and metal oxides as discussed in previous section. In the precursor heated continuously without intermediate cooling from 300 to 800°C, the XRD pattern (Fig. 2c) shows the presence of mainly the 2212 phase along with other oxides identified as 2201, CuO and Ca_2CuO_3. It is worth mentioning that the precursor which was heated with intermediate cooling from 300 (2 h and then cool) to 800°C still showed the evidence of the carbonates in the oxide powder.

The formation of 2212 may be explained by the sequence of reactions given as:

$$2CaO+CuO \rightarrow Ca_2CuO_3 \quad (1)$$

followed by

$$2(2201)+Ca_2CuO_3+CuO \rightarrow 2(2212) \quad (2)$$

It follows from Fig. 2d that major phase in the sample sintered at 845°C is 2212. There is no change in the basic XRD patterns as compared to oxide powder (Fig. 2c) other than the peaks of CuO were reduced in the sintered sample and those for Ca_2CuO_3 increased. This also shows the stability of 2212 phase in the BSCCO material. It is anticipated that stronger peaks from 2212 phase in the sintered material appeared because of grain growth and enhanced crystallization of this phase during sintering process. From the XRD pattern (Fig. 2e), it is evident that major phases are 2212 and 2223 and minor phases are 2201 and CuO in the sample sintered at 860°C. The Ca_2CuO_3 phase was not observed at 860°C. These results indicated that the 2223 phase required a complex dissolution–diffusion precipitation process for its formation. Liquid phase sintering [44] at 860°C is shown to aid the formation of the 2223 phase. It has been proposed [45] that an interface was created between 2212 phase and Ca_2CuO_3 during the crystallization of the system. Because of the high concentration difference in Ca and Cu across the interface, dif-

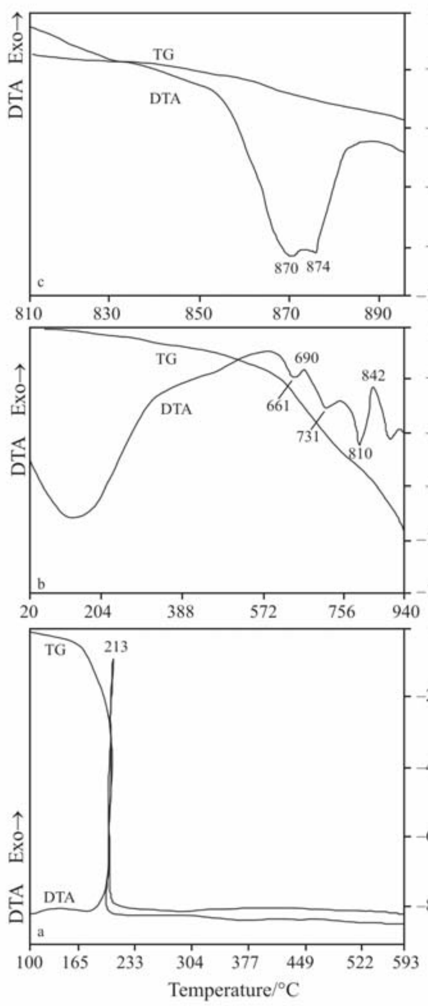

Fig. 3 Thermal analysis (TG/DTA) of a – EDTA gel, b – precursor calcined at 300 and c – at 800şC

fusion of Ca and Cu atoms towards the 2212 phase occurred at elevated temperature. The 2223 phase grew at these interfaces as appreciable amounts of Ca and Cu diffused into the 2212 phase. XRD results indicate that on increasing the sintering temperature from 845 to 860°C, the amounts of the 2212, 2201 phases and the compounds containing Ca and Cu decreased. The 2212 phase transformed to 2223 phase after Ca and Cu from Ca_2CuO_3 and CuO had diffused into the 2212 phase.

Thermal and shrinkage analysis

Figures 3a–c show the TG/DTA curves for the EDTA gel, precursor heated at 300 and 800°C. TG curve Fig. 3a revealed that after the initial loss of water, a single sharp mass loss occurred and the precursor decomposed almost completely at 230°C (DTA curve) with a major mass loss. The breaking up of the organic complex, volatilization of NH_4NO_3, elimination of nitrate ions and free EDTA, contributed to this stage. Figure 3b shows the TG/DTA curves of the precursor calcined at 300°C for 2 h. The thermal curve indicated that the mass loss started below 200°C and completed above 850°C with multiple intermediate decomposition reaction as shown in DTA curve. These decomposition reactions may be attributed to the formation of carbonates and superconducting phases. These observations support the FTIR and XRD results discussed earlier. It can be seen from Fig. 3c that there is no any peak below the temperature 850°C. It is revealed that the formation of carbonates can be suppressed by heating the gel precursor continuously without intermediate cooling from 300 to 800°C.

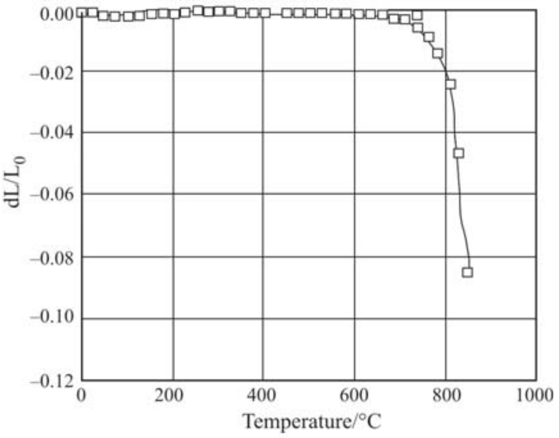

Fig. 4 Dilatometry curve for the precursor calcined at 800°C

Figure 4 shows the dilatometry curve of the oxide powder which was pressed and sintered. The curve shows the change in length during sintering of pressed pellets. There was no change in length on heating up to a temperature of 600°C. However, a large shrinkage occurred as a result of sintering between 700 and 800°C. This was equivalent to 2.2% reduction from the original length. This shrinkage as a result of sintering, occurred at an even increasing rate as heating was continued between 800 and 850°C. This was equivalent to 1.2% reduction from the original sample length. Above 850°C, the sample can be seen to shrink drastically up to a temperature of 865°C. This temperature could be partial melting temperature of the material. The evidence for partial melting could be gained from deformed appearance of the sample where the push rod of the dilatometer assembly had indented the specimen.

On the basis of dilatometry results, the pellets of the powder were pressed and sintered at 845 and 860°C in order to observe the formation of superconducting phases. The formation of different superconducting phases has already been discussed in the previous section.

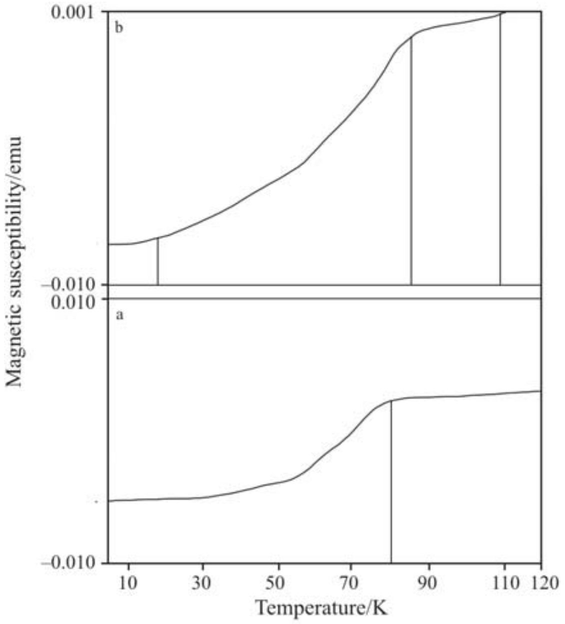

Fig. 5 Magnetic susceptibility behavior of sample sintered at a – 845 and b – 860°C for 60 h

Superconducting properties of sintered products

Figures 5a and b show the relationship between AC magnetic susceptibility and temperature for the sample sintered at 845 and 860°C for 60 h. Figure 5a indicates the presence of 2212 phase with a transition at 80 K in the sample sintered at 845°C. Figure 5b gives the clue of 2223 phase with T_c of 108 K in the sample sintered at 860°C. However, the major superconductivity is seen with a step at 85 K which reveals the main phase to be 2212 as confirmed by XRD results.

Conclusions

- For the preparation of precursor of desirable properties, pH is the deciding factor.
- Although NH_4NO_3 precipitates during gel drying, it does not cause any chemical inhomogeneity or agglomeration in the final superconducting phases because it does not involve any metal ion.
- EDTA gel decomposed in single step, whereas the precursor calcined at 300°C showed a number of decomposition steps. There is no any decomposition steps observed in TG/DTA curves before 850°C in the precursor calcined at 800°C.
- No change in length was observed in case of dilatometry up to a temperature of 600°C, however a large shrinkage was noted above 700°C.
- The dominant phase for oxide powder sintered at 845°C for 120 h is 2212 whereas it is 2223 for the same sample sintered at 860°C for 60 h.
- The study inferred that formation of 2223 phase involves a complex dissolution–diffusion precipitation mechanism.

Acknowledgements

We owe special thanks to Messrs. Nadeem Ahmed, Shahid Mahmood, Gulzar Ali and Saeed-ul-Hasan, for their unflagging, enthusiastic and capable cooperation throughout our research work.

References

1 B. Simendic and L. Radonjic, J. Therm. Anal. Cal., 79 (2005) 487.
2 M. Picquart, T. Lopez, R. Gomez, E. Torres, A. Moreno and J. Garcia, J. Therm. Anal. Cal., 76 (2004) 755.
3 V. Balek, Z. Malek, J. Subrt, M. Guglielmi, P. Innozenzi, V. Rigato and G. Della Mea, J. Therm. Anal. Cal., 76 (2004) 43.
4 A. Biju, R. P. Aloysius and U. Syamaprasad, Supercond. Sci. Technol., 18 (2005) 1454 and references therein.
5 K. Gibson, P. Ziegler and H.-J. Meyer, Supercond. Sci. Technol., 17 (2004) 786.
6 P. Staszczuk, D. Sternik and G. W. Chadzymski, J. Therm. Anal. Cal., 71 (2003) 173.
7 T. Ozawa, J. Therm. Anal. Cal., 72 (2003) 337.
8 R.Campostrini, M. Ischia and L. Palmisano, J. Therm. Anal. Cal., 71 (2003) 1011.
9 L. Ammor, B. Pignon, N. H. Hong and A. Ruyter, Supercond. Sci. Technol., 17 (2004) 1037.
10 D. A. M. dos Santos, S. Mochlecke, Y. Kopelevich and A. J. S. Machado, Physica C, 390 (2003) 21.
11 G. A. Cosla, A. Ubaldini, C. Astini, M. M. Carnasciali and R. Masini, J. Therm. Anal. Cal., 80 (2005) 579.
12 M. A. Aksan, M. E. Yakinci and Y. Balci, J. Therm. Anal. Cal., 81 (2005) 417.
13 A. Y. Iiyusheshkin, Y. Yamashita, L. Boskorie and I. D. Mackinnon, Supercond. Sci. Technol., 17 (2004) 1201.
14 P. Sumana Prabu, M. S. Ramachandra, U. V. Varadaraju and G. V. Subbha Rao, Phys. Rev. B, 50 (1994) 6929.
15 F. Nakao and K. Osamura, Supercond. Sci. Technol., 18 (2005) 513.
16 L. Ammor, B. Pignon, N. H. Hong and A. Ruyter, Supercond. Sci. Technol., 17 (2004) 1037.
17 A. Caneiro, F. Prado and A. Serquis, J. Therm. Anal. Cal., 83 (2006) 507.
18 S. Räth, L. Woodall, C. Deroche, B. Seipel, F. Schwaigerer and W. W. Schmahl, Supercond. Sci. Technol., 15 (2002) 543.
19 H. Cooper, S. Li, W. Gao, H. K. Liu and S. X. Dou, Supercond. Sci. Technol., 14 (2001) 533.
20 M. Arshad and A. H. Qureshi, J. Therm. Anal. Cal., 83 (2006) 415.
21 C. Marcilly, P. Courty and B. Delmon, J. Am. Ceram. Soc., 53 (1970) 56.
22 M. S. G. Baythoun and F. R. Sale, J. Mater. Sci., 17 (1982) 2757.
23 D. J. Anderton, Powder Metallurgy, (1979) 14.
24 C. T. Chu and B. Dunn, J. Am. Ceram. Soc., 70 (1987) C375.

25 H. W. Wang, D. A. Hall and F. R. Sale, J. Am. Ceram. Soc., 75 (1992) 124.

26 J. Fransaer, J. R. Roos, L. Delaey, O. Van Der Biest, O. Arkens and J. P. Celis, J. Appl. Phys., 65 (1989) 3277.

27 V. D. Biest, Proc. 1st European Ceramic Society Conf. J.2, Elsevier Applied Science, June (1989) 407.

28 G. C. Tu, F. H. Chen and H. S. Koo, Supercond. Sci. Technol., 3 (1990) 134.

29 U. Kuxmann and P. Fischer, Erzmetall, 27 (1974) 533.

30 A. Aoki, Jap. J. Appl. Phys., 29 (1990) L270.

31 T. S. Heh, J. R. Chen and T. Y. Tseng, Jpn. J. Appl. Phys., 29 (1990) 652.

32 N. H. Wang, C. M. Wang, H. C. Kao, D. C. Ling, H. C. Ku and K. H. Lii, Jpn. J. Appl. Phys., 28 (1989) L1505.

33 F. R. Sale and F. Mahloojchi, Ceramics Int., 14 (1988) 229.

34 B. Delmon, Fine Particles, Second Int. Conference Ed. by W. E. Kuhn and J. Ehretsmann (The electrochemical Soc. New Jersey) PV, 73 (1974) 242.

35 A. J. Moulson and J. M. Herbert, Eds, Electroceramics, 2nd Edition, John Willey and Son Ltd., 2003.

36 A. H. Qureshi, M. Arshad, K. Masud and A. Saeed, J. Therm. Anal. Cal., 81 (2005) 363.

37 A. H. Qureshi, S. K. Durani, M. Arshad, F. R. Sale, N. Arshad and S. Rehman, J. Chem. Soc. Pak, 25 (2003) 177.

38 C. B. Alcock and B. Li, J. Am. Ceram. Soc., 73 (1990) 1176.

39 A. D. Cross, Introduction to Practical Infrared Spectroscopy, Bros. Norschich Ltd., 1960.

40 The Sadtler Standard Spectra, Sadtler Research Laboratories, Philadelphia, PA 1974, p. 5.

41 E. Pungor, A Practical Guide to Instrumental Analysis CRC Press, (1994) 163.

42 P. C. Srivastava, B. N. Singh, S. D. Adhya and K. C. Banerji, J. Thermal Anal., 27 (1983) 263.

43 J. Paulik and F. Paulik, Simultaneous Thermoanalytical Examinations by Means of the Derivatograph in Wilson and Wilson's Comprehensive Analytical Chemistry, Svehla G. Ed. Elsevier, Amsterdam 1981, p. 12A.

44 Y. Ikeda, H. Ito, S. Shimomura, M. Takano, Y. Bando, J. Takada, K. Oda, H. Kitaguchi, Y. Miura, Y. Takeda and T. Takada, Physica C, 190 (1991) 18.

45 D. Shi, M. Tang, K. Vandevoot and H. Claus, Phys. Rev. B, 39 (1989) 9091.

Received: February 20, 2006
Accepted: May 31, 2006
OnlineFirst: October 20, 2006

DOI: 10.1007/s10973-006-7538-x